Refereed Proceedings

The 13th International Conference on Fluidization - New Paradigm in Fluidization Engineering

---

Engineering Conferences International *Year* 2010

EXPERIMENTS AND MODELLING OF MICRO-JET ASSISTED FLUIDIZATION OF NANOPARTICLES

J. Ruud van Ommen* David M. King† Alan Weimer‡
Robert Pfeffer** Berend van Wachem††

*Delft University of Technology, j.r.vanommen@tudelft.nl
†University of Colorado Boulder, david.m.king@colorado.edu
‡University of Colorado Boulder, alan.weimer@colorado.edu
**Arizona State University, robert.pfeffer@asu.edu
††Imperial College London, b.van-wachem@imperial.ac.uk

EXPERIMENTS AND MODELLING OF MICRO-JET ASSISTED FLUIDIZATION OF NANOPARTICLES

J. Ruud van Ommen
Department of Chemical Engineering, Delft University of Technology
Julianalaan 136, 2628 BL Delft, The Netherlands
T: +3115 278 2133; F: +3115 278 5006; E: j.r.vanommen@tudelft.nl

David M. King and Alan Weimer
Department of Chemical and Biological Engineering, University of Colorado
Boulder, CO 80309-0424, USA
david.m.king@colorado.edu; alan.weimer@colorado.edu

Robert Pfeffer
Department of Chemical Engineering, Arizona State University
Tempe, AZ 85287, USA
robert.pfeffer@asu.edu

Berend G.M. van Wachem
Department of Mechanical Engineering, Imperial College London
Exhibition Road, London SW7 2AZ, United Kingdom
B.van-wachem@imperial.ac.uk

ABSTRACT

The fluidization of nanoparticle agglomerates can be largely improved by using downward pointing micronozzles, creating a high-velocity jet, as experimentally shown. By discrete particle simulations – treating the agglomerates as single particles – we show that the main reason is probably the reduction of the agglomerate size by agglomerate-agglomerate collisions.

INTRODUCTION

Fluidization of nanoparticles has gained a lot of interest in recent years. It poses challenging scientific questions, but also has practical applications. For example, through atomic layer deposition it is possible to provide individual nanoparticles with an ultrathin coating. Weimer and co-workers demonstrated this technique for a wide variety of materials (1,2,3); recently van Ommen and co-workers showed that it is possible to carry out the process at atmospheric pressure (4). Although it sounds counterintuitive that nanoparticles could be fluidized, it is possible since nanoparticles form agglomerates with sizes in the order of 100 μm. These agglomerates are so dilute – they are often assumed to have a fractal nature – that coating individual nanoparticles is possible. In the past years, several researchers have made efforts to model the formation and fluidization of agglomerates (see, e.g., 5,6,7,8). Because of the large cohesive forces, it is often needed to assist the fluidization of nanoparticles. Several ways have been proposed, such as vibration, sound wave pulsation, and the use of AC electric fields (9). Recently, Quevedo et al. (10) proposed the use of microjets as an alternative. They showed that the fluidization behaviour of nanoparticle agglomerates is greatly enhanced by adding a secondary flow in the form of a high-velocity jet produced by one or more micronozzles pointing vertically downward toward the distributor. The micronozzles produced a jet with high velocity (hundreds of meters per second), breaking up large nanoagglomerates, preventing channelling, curtailing bubbling, and promoting liquid-like fluidization. In addition, they claimed that microjet-assisted nanofluidization was also found to improve solids motion and prevent powder packing in an internal, is easily scaled-up, and can mix and blend different species of nanoparticles on the nanoscale. They proposed that microjets improve the fluidization by increasing the turbulence and inducing high shear forces, which lead to agglomerate breakage. In this paper, we aim at achieving a further elucidation of the mechanisms through which a microjet enhances nanoparticle fluidization using experiments and modelling.

APPROACH

Experimental

Experiments are carried out in a glass column with a diameter of 32 mm, equipped with a 10 μm porous stainless steel distributor plate and outlet filters (Mott Corporation, Farmington, CT); the distributor plate is 1.6 mm thick. Metal face-seal conflat flanges were welded to the top and bottom of each reactor tube and sealed using copper gaskets. VCR® (Swagelok Co., Solon, OH) adaptors were welded to the outer flanges at the inlet and outlet of the reaction vessel. The bed material consists of 25 nm TiO2 particles, which tend to form soft agglomerates. The settled bed height is 114 mm. A downward pointing tube is inserted at the axis of the column; at the end of the tube a micro-nozzle with an internal diameter of 128 μm has been attached. The bed is fluidized at atmospheric pressure and room temperature with nitrogen at superficial gas velocities ranging from 0 to 0.12 m/s. Through the nozzle, we apply a nitrogen flow with a velocity of 300 m/s, corresponding to a superficial gas velocity of 0.0048 m/s.

Modelling

For the modeling of particles and fluids, different approaches and models exist, depending on the scale and region of interest. A true DNS model (e.g. Lattice Boltzmann or immersed boundary) can be used to determine the flow around individual particles, while a discrete particle or element method (DPM/DEM) or CFD-DEM is able to simulate a larger number of particles, by approximating them as point sources for the fluid phase. If the system size is increased further, the particle phase is treated as a continuous phase: Eulerian-Eulerian modeling. Even larger systems can be simulated by the discrete bubble model, which has a continuous particle phase with each bubble modeled separately.

In this research, the interaction between the fluid and the particle agglomerates is of interest. Therefore, a CFD-DEM (Eulerian-Lagrangian) model was chosen. In this model, the fluid is represented as a continuous medium. Since agglomerates consist of millions up to billions of nanoparticles, it is not possible to model each individual nanoparticle. Instead, we model the agglomerates as spheres with a typical density and diameter that has been found experimentally in previous studies (6,8). For simplicity, we assumed all agglomerates to have the same size, and we did not include the breakage of agglomerates. Although we realize that this is a rough approximation, we think this approach is a good first step to obtain insight in the forces that are exerted on the nanoparticle agglomerates. We intend to extend the model to e.g. include agglomerate breakage in the near future. The program that was used is MultiFlow (11). Gas-agglomerate interactions (drag force) are calculated by the Wen and Yu correlation (12). Agglomerate-agglomerate interactions are calculated using the soft-sphere approach. This type of modeling enables multiple collisions, which occur frequently in a dense fluidized bed. When agglomerates collide, they will have a reversible deformation, leading to a repulsive force between the agglomerates. The elastic deformation is approximated by allowing a small overlap, and a repulsive force model is based upon the magnitude of the overlap. The model is based upon the pioneering work of Mindlin and Deresiewicz (13) and Tsuji et al. (14). Model details and implementation can de found in Hemph et al. (15). The agglomerate motion is calculated by integrating Newton's law of motion and the fluid is modeled by approximating the Navier-Stokes equations in a finite volume discretized framework.

Table 1: Agglomerate parameters

Property	Value
Model type	Lagrangian
Diameter	260 µm
Density	30 kg/m^3
Youngs modulus	5·10^5 GPa
Coef. of restitution	0.9
Poisson ratio	0.25
Coef. Of Friction	0.35
Number of agglom.	260,000

Table 2: System settings

Property	Value
Steps per collision	36
Time step hydrodynamics	1·10^{-4} s
Gravitation constant	10 m/s^2
X-dimension	30·10^{-3} m
Y-dimension	4·10^{-3} m
Z-dimension	100·10^{-3} m
Superficial gas velocity	2.0·10^{-2} m/s

The most important properties of the agglomerates are shown in Table 1. A value of 5.5·10^5 GPa is used for the Young modulus. The minimum fluidization velocity for these agglomerates was calculated to be 0.6 mm/s, using the Wen and Yu correlation (12). Note, however, that the Wen and Yu correlation has not been validated for particles (agglomerates) with such a low density. The properties of the walls with respect to collision are equal to the agglomerates' properties. The fluid is air at ambient conditions with a temperature of 298.15 K and a pressure of 1·10^5 Pa. The density of air is 1.21 kg/m^3 and the viscosity 1.52·10^{-5} Pa· s.

The other simulation settings are given in Table 2. The time steps for the particle phase in the model are determined by the collisions. Each collision is calculated in 36 steps and depending on the collision properties, such as velocities and masses, a time step is calculated. The jet tip is positioned in the centre of the horizontal cross-section at $100\cdot10^{-3}$ m above the distributor; the jet is pointing downward. The mesh is refined around the microjet. We carried out two different simulations: a base case with a superficial gas velocity of $2.0\cdot10^{-2}$ m/s and the jet turned off, and a second simulation with a superficial gas velocity of $1.4\cdot10^{-2}$ m/s through the distributor and a gas velocity of 18 m/s through the jet. The horizontal cross-section of the jet is 200 μm x 200 μm. The total amount of gas provided to the bed is equal for the two cases.

RESULTS AND DISCUSSION

Experiments

In the experiments, visually a strong increase of the bed height was observed; Fig. 1 shows that a bed expansion with a factor 2.5 has been observed. In this case, the gas velocity of the jet nozzle was 300 m/s. This would lead to a particle Reynolds number of 5200 (see Eq. (1)), well above the threshold for full turbulence for the particle Reynolds number. However, the gas will quickly be dispersed and slowed down in the region below the jet nozzle: there will only be a very small part of the bed experiencing turbulence. This makes it unlikely that turbulence is the main explanation of the decrease of agglomerate size leading to the strong bed expansion. Possible other explanations will be investigated using the simulation results.

$$\mathrm{Re_p} = \frac{\rho v d}{\mu} = \frac{1.2\cdot300\cdot260\cdot10^{-6}}{1.8\cdot10^{-5}} = 5200 \qquad (1)$$

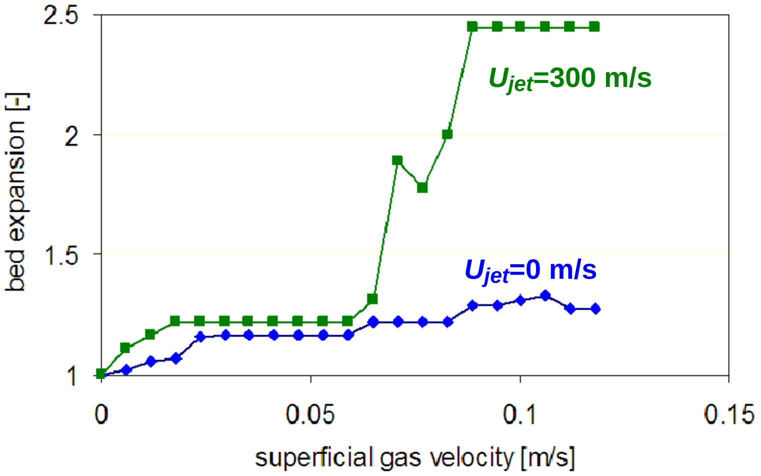

Figure 1. Bed expansion as a function of the superficial gas velocity with and without a jet flow.

Simulations

With the simulations, it is not possible to mimic the experimental set-up completely: the amounts of nanoparticles agglomerates would become too large (>10^6) to keep the computational times within reasonable limits. Therefore, we decided to study a pseudo 2D geometry. The depth is limited (4 mm), but large enough in term of agglomerate diameters (>10 times the agglomerate diameter). For the simulations, the ratio of the microjet cross-section (200 μm x 200 μm) compared to the bed cross-section (30 mm x 4 mm) is much larger than in the experimental setup (3.3 x 10^{-4} versus 1.6 x 10^{-5}). In order to keep the volumetric flow rate through the jet in the advised range (10-30% of the total volumetric flow rate), we used a much lower jet velocity in the simulations (18 m/s). In spite of these differences between the experimental setup and the simulations, we still expect to obtain qualitative insight in the mechanisms in which the jet enhances the fluidization of nanoparticle agglomerates.

The simulations have been run for a period of 2 s of real time. The first second has been discarded to ensure stationary behaviour. Over the period from one to two seconds, we have calculated average values to get a first impression of the hydrodynamics. We show the results in colour contour plots in a vertical cross section through the middle of the fluidized bed. Figure 2 shows the voidage distribution over the bed. It is remarkable that whether the jet is on or off does not seem to influence the voidage distribution strongly. There is no low voidage region at the tip of the jet, but the differences between low- and high-voidage regions and the asymmetry in the bed seem somewhat larger in the case when the jet is on. The asymmetry in the profiles is most probably due to the short simulation times: over a period of several seconds a more even distribution is expected. The most important

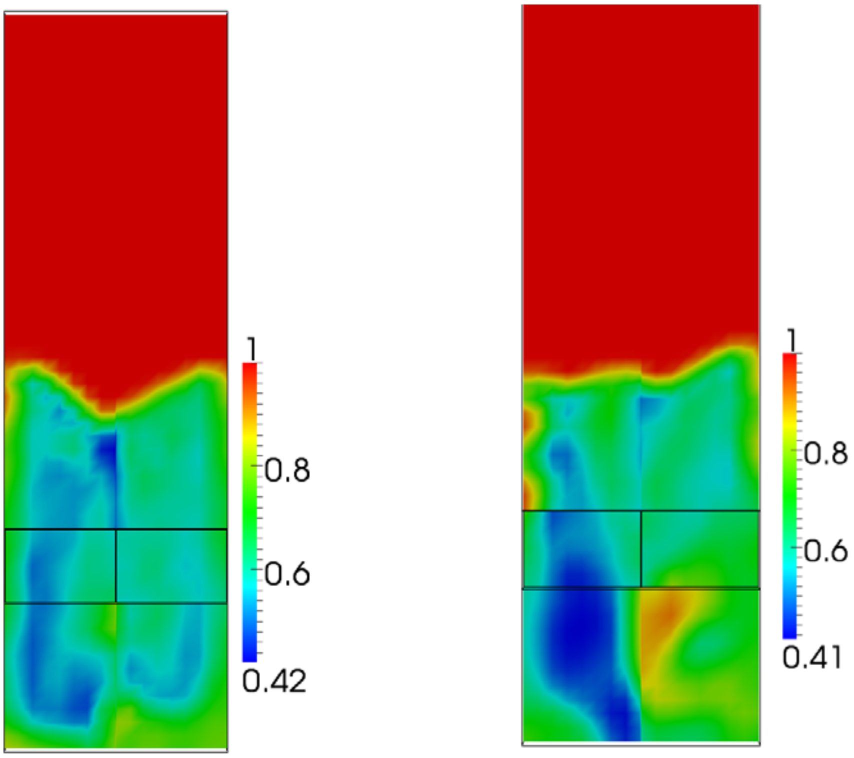

Figure 2. The voidage as a function of the position in the bed for (a) the jet turned off and (b) the jet turned on.

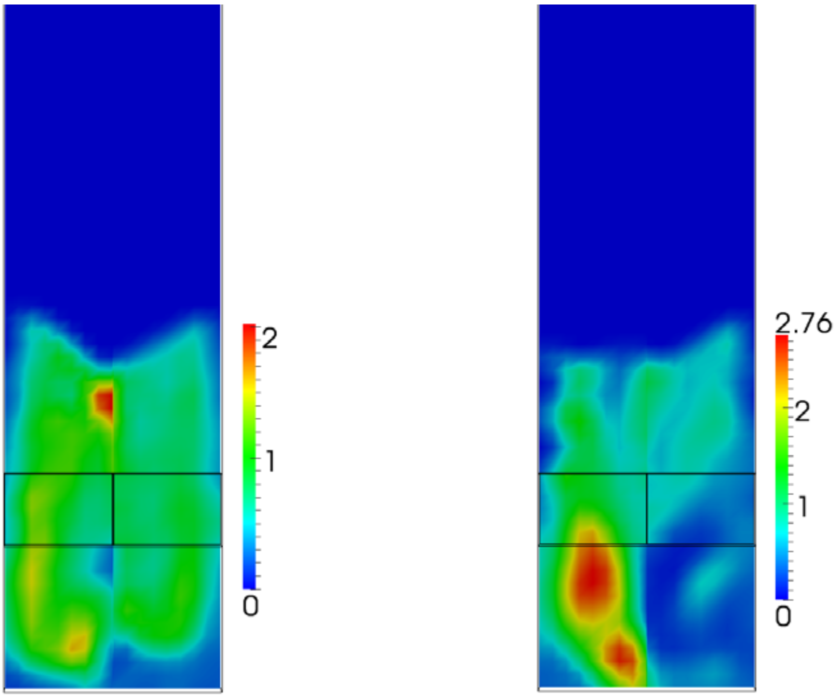

Figure 3. The drag force [N] as a function of the position in the bed for (a) the jet turned off and (b) the jet turned on.

conclusion that we can draw from the voidage plots is that the bed height in both cases is the same. This means that the high jet velocity itself does not lead to the large bed expansion, but the agglomerate breakage resulting from the action of the jet. Since these simulations assume a constant agglomerate size (i.e. agglomerate breakage is not considered), no bed height increase is observed.

The distribution of the drag force over the bed is, as expected, largely in agreement with the voidage distribution (see Fig. 3): there is some difference between the case without and with the jet, but in both cases the drag force remains of the same order of magnitude. This means that shear is probably not the most important phenomenon leading to the agglomerate size reduction that is experimentally observed.

Figure 4 shows the collisional stress as a function of the position in the bed. These plots show for the case of the jet turned the presence of a region with very high collisional stresses below the jet: the stresses in this region are one to two orders of magnitude larger than in the case without a jet. This demonstrates that agglomerate-agglomerate collisions are probably the main reason for agglomerate size reduction in a jet-assisted fluidized bed. However, it should be taken into account that – in order to keep the computational effort within limits – these simulation have been carried out in a pseudo 2D-geometry, while all experimental work with micro-jets up to now has been carried out with cylindrical columns.

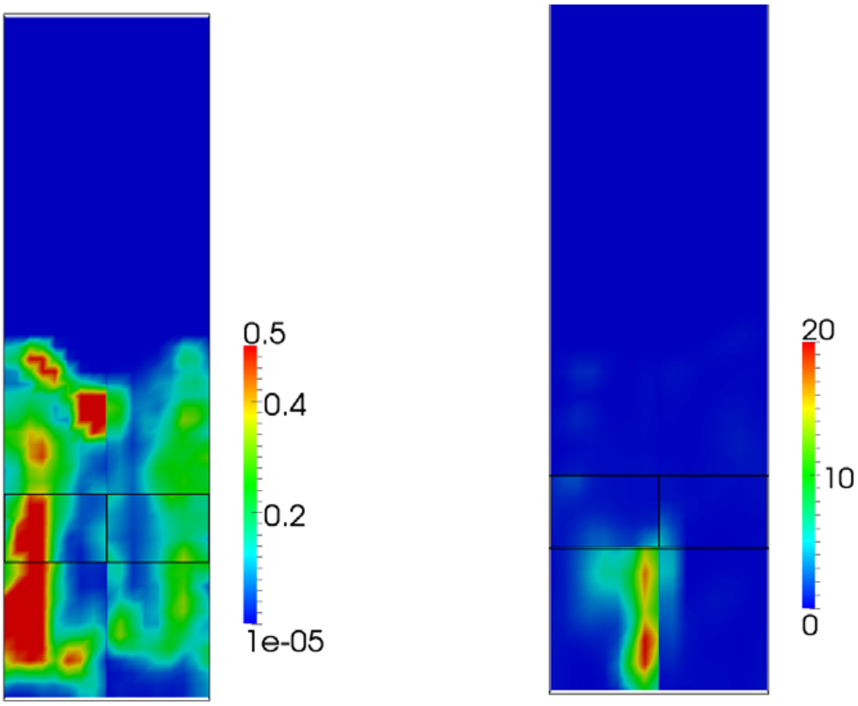

Figure 4. The collisional stress [Pa] as a function of the position in the bed for (a) the jet turned off and (b) the jet turned on.

CONCLUDING REMARKS

Experiments have shown that the fluidization behaviour of nanoparticle agglomerates is greatly enhanced by adding a secondary flow in the form of a high-velocity jet produced by one or more micronozzles pointing vertically downward toward the distributor. This paper shows just one set of experiments in a cylindrical column, but elsewhere a much larger amount of data can be found. These microjets improve the fluidization via a break-up of the agglomerates. The corresponding particle Reynolds numbers make it questionable if the turbulence plays a large role in this process. Discrete particle simulations for a pseudo 2D geometry, in which the agglomerates are mimicked by single particles, show some increase in the drag force on the agglomerates by adding a microjet. However, the largest contribution to the agglomerate size reduction seems to come from agglomerate-agglomerate collisions: the collisional stress in the zone below the jet is one to two orders of magnitude larger than for the case without a jet.

ACKNOWLEDGEMENTS

We would like to thank Alia Lubers and Sam Johnson for their assistance in the experimental work.

REFERENCES

1. Hakim, L. F., Blackson, J., George, S. M., Weimer, A. W. (2005), ‘Nanocoating individual silica nanoparticles by atomic layer deposition in a fluidized bed reactor’, Chem. Vap. Deposition **11**, 420-425.
2. King, D.M., Johnson, S.I., Li, J., Du, X., Liang, X., Weimer, A.W. (2009), ‘Atomic layer deposition of quantum-confined ZnO nanostructures’, Nanotechnology **20,** 195401.
3. Liang, X., King, D.M., Li, P., George, S.M., Weimer, A.W. (2009), ‘Nanocoating hybrid polymer films on large quantities of cohesive nanoparticles by molecular layer deposition ’, AIChE J. **55**, 1030-1039.
4. Beetstra, R., Lafont, U., Nijenhuis, J., Kelder, E.M., van Ommen, J.R. (2009), ‘Particle coating by Atomic Layer Deposition: protection of cathode material for Li-ion batteries against degradation’, Chem. Vap. Deposition **15**, 227 - 233.
5. Chaouki, J., Chavarie, C. Klvana, D., Pajonk, G. (1985), ‘Effect of interparticle forces on the hydrodynamic behaviour of fluidized aerogels’, Powder Technol. **43**, 117-125.
6. Yao, W., Guangsheng, G., Fei, W., Wu, J. (2002), ‘Fluidization and agglomerate structure of SiO_2 nanoparticles’, Powder Technol. **124**, 152–159.
7. Jung, J. and D. Gidaspow (2002), ‘Fluidization of nano-size particles’, J. Nanopart. Res. **4**, 483-497.
8. Hakim, L.F., Portman, J.L., Casper, M.D., Weimer, A.W. (2005), ‘Aggregation behavior of nanoparticles in fluidized beds’, Powder Technol. **160**, 149-160.
9. Lepek, D., Valverde, J.M., Pfeffer, R., Dave, R.J. (2010), ‘Enhanced nanofluidization by alternating electric fields’, AIChE J. **56**, 54-65.
10. Quevedo, J.A., Omosebi, A., Pfeffer, R. (2010), ‘Fluidization enhancement of agglomerates of metal oxide nanopowders by microjets’, AIChE J., in press, DOI: 10.1002/aic.12075.
11. Van Wachem, B.G.M. (2008) MultiFlow - A fully coupled solver for multiphase flows, www.multiflow.org
12. Wen, C., Yu, Y. (1966), ‘Mechanics of fluidization’, Chemical engineering programming symposium **62**, 100-110.
13. Mindlin, R., Deresiewicz, H. (1953), ‘Elastic spheres in contact under varying oblique forces’, J. Appl. Mech. **20**, 327-344
14. Tsuji, Y., Kawaguchi, T., Tanaka, T. (1993), ‘Discrete particle simulation of two-dimensional fluidized bed’, Powder Technol. **77**, 79-87
15. Hemph, R., van Wachem, B., and Almstedt, A.-E. (2006), ‘Distinct element modeling of hopper flows comparison and validation of models and parameters’, In: Proc. Fifth World Congress on Particle Technology, Orlando, Florida.

EXPERIMENTS AND MODELLING OF MICRO-JET ASSISTED FLUIDIZATION OF NANOPARTICLES

J. Ruud van Ommen, David M. King, Alan Weimer, Robert Pfeffer, Berend G.M. van Wachem

KEYWORDS

Nanoparticles, agglomerates, microjet, jet, assisted fluidization, discrete particle modelling.